International Journal of Solids and Structures 51 (2014) 2261–2271

Contents lists available at ScienceDirect

International Journal of Solids and Structures

journal homepage: www.elsevier.com/locate/ijsolstr

A simple and efficient BEM implementation of quasistatic linear visco-elasticity

C.G. Panagiotopoulos [a], V. Mantič [a,*], T. Roubíček [b,c]

[a] Group of Elasticity and Strength of Materials, Department of Continuum Mechanics School of Engineering, University of Seville, Camino de los Descubrimientos s/n, ES-41092 Sevilla, Spain

[b] Mathematical Institute, Charles University, Sokolovská 83, CZ-18675 Praha 8, Czech Republic

[c] Institute of Thermomechanics of the ASCR, Dolejškova 5, CZ-18200 Praha 8, Czech Republic

ARTICLE INFO

Article history:
Received 7 August 2013
Received in revised form 8 February 2014
Available online 28 February 2014

Keywords:
Boundary element method
Implicit time discretisation
Quasistatic linear visco-elasticity
Unilateral contact
Kelvin–Voigt rheology
Maxwell rheology
Standard linear solids
Jeffreys rheology
Burgers rheology

ABSTRACT

A simple yet efficient procedure to solve quasistatic problems of special linear visco-elastic solids at small strains with equal rheological response in all tensorial components, utilizing boundary element method (BEM), is introduced. This procedure is based on the implicit discretisation in time (the so-called Rothe method) combined with a simple "algebraic" transformation of variables, leading to a numerically stable procedure (proved explicitly by discrete energy estimates), which can be easily implemented in a BEM code to solve initial-boundary value visco-elastic problems by using the Kelvin elastostatic fundamental solution only. It is worth mentioning that no inverse Laplace transform is required here. The formulation is straightforward for both 2D and 3D problems involving unilateral frictionless contact. Although the focus is to the simplest Kelvin–Voigt rheology, a generalization to Maxwell, Boltzmann, Jeffreys, and Burgers rheologies is proposed, discussed, and implemented in the BEM code too. A few 2D and 3D initial-boundary value problems, one of them with unilateral frictionless contact, are solved numerically.

1. Introduction

A large number of engineering and (e.g. geo-) physical applications consider materials that exhibit *visco-elastic behavior*. A typical example of such a behavior is the mechanical response of polymers and polymer-matrix composites, or rocks undergoing aseismic slip, etc. Visco-elasticity accounts for the dependence of stresses and strains on time, and response of real visco-elastic solids or structures is usually analyzed numerically by the finite or boundary element methods (FEM or BEM). When inertial effects are neglected, usually because of sufficiently slow external loading, the model is addressed as *quasistatic*. The quasistatic linear visco-elasticity theory provides a usable engineering approximation for many applications in polymer and composites engineering, among others. There are several models describing visco-elastic behavior of materials obtained by a generalization of simple 1D models to 2D or 3D ones. One of these well-known models, often adopted in designing procedures, is the Kelvin–Voigt model.

There are four main approaches to *quasistatic linear visco-elastic analysis by BEM*. The first and most commonly applied approach uses the correspondence principle to establish an associated elastic problem solved in the Laplace transform domain. Then, the solution in time domain is recovered by a numerical inversion (Rizzo and Shippy, 1971; Manolis and Beskos, 1981; Kusama and Mitsui, 1982; Sládek et al., 1984; Carini and Gioda, 1986; Chen and Hwu, 2011). The second approach works directly in the time domain, however, it requires a time dependent fundamental solution (Lee and Westmann, 1995; Cezario et al., 2011; Zhu et al., 2011). The third, a kind of mixed, approach also solves the problem in time domain, but uses the Laplace transformed fundamental solutions with a convolution quadrature leading to a time stepping procedure without the knowledge of the time dependent fundamental solution (Schanz, 1999; Schanz et al., 2005; Syngellakis and Wu, 2004). The fourth, a kind of direct, approach which utilizes the Kelvin elastostatic fundamental solution was introduced by Mesquita et al. (2001) and Mesquita and Coda (2002) for both Kelvin–Voigt and Boltzmann visco-elastic models. The Somigliana displacement and stress identities are rewritten to obtain *visco-elastic boundary-integral-representations* (BIRs) for these models. After the BEM discretisation of these BIRs, a *finite difference approximation* of velocities leads to a time marching scheme. This approach was later applied to the problem of circular holes and elastic inclusions in a visco-elastic plane (Huang et al., 2005a,b).

* Corresponding author. Tel.: +34 954 482135; fax: +34 954 461637.
E-mail address: mantic@us.es (V. Mantič).

http://dx.doi.org/10.1016/j.ijsolstr.2014.02.028
0020-7683/

A brief presentation of several BEM procedures for problems of visco-elasticity may be found in Marques and Creus (2012).

The novelty of the present approach consists in a particular application of the Rothe method (i.e. the time discretisation by the implicit Euler formula, cf. e.g. Roubíček, 2013a) to the governing partial differential equations (PDE), where after this time discretisation, a suitable variable transform is carried out to convert it in each time step to an *auxiliary linear elastostatic problem* with proper boundary conditions. Once this linear elastostatic problem is solved the actual displacements, stresses and strains of the visco-elastic problem in this time step are recovered and used in the next step, an efficient recursive procedure being obtained in this way. For the sake of simplicity of explanation, the main steps of the procedure proposed are first explained for the simple Kelvin–Voigt model, and then briefly generalized to other basic linear visco-elastic rheologies. The present procedure can be implemented in any elastostatic FEM or BEM code. The present work is based on the collocation BEM formulation due to its advantages as no domain variables appear in the solution of the problem. Additionally the stability of the present time discretisation can be established. Although there are evident similarities with the previous work by Mesquita and Coda, the present theoretical formulation is much straightforward, showing in a more transparent way that any linear elastostatic BEM code can be applied to a linear visco-elastic analysis requiring just minor modifications.

Under the above mentioned assumptions, the purpose of this work is to present and numerically verify a simple yet efficient methodology for BEM analysis of quasistatic visco-elastic problems, initially scrutinizing the Kelvin–Voigt material in Sections 2 and 3 and later, in Section 4, further extended to other models usually found in engineering or physical applications. The approach may be considered as a time domain one, where no special time-depended fundamental solution, neither domain integration, is needed. Another important engineering problem treated in this work is a contact of visco-elastic bodies (Graham, 1965).

2. The mixed unilateral initial-boundary-value problem for Kelvin–Voigt visco-elastic body

The following boundary-value problem on a domain $\Omega \subset \mathbb{R}^d$, $d = 2, 3$, is used in the subsequent developments, where also the standard model of the frictionless unilateral Signorini contact is considered, see Fig. 1,

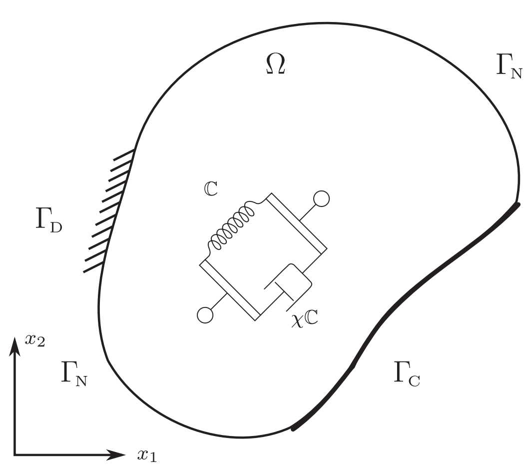

Fig. 1. 2D schematic illustration of the geometry and notation of the boundary-value problems considered. In the bulk, a visco-elastic rheology from Fig. 2 is schematically depicted.

$$\operatorname{div} \mathbb{C}\epsilon + f = 0 \quad \text{with} \quad \epsilon = \epsilon(u, \dot{u}) = e(u + \chi\dot{u}) \quad \text{on } \Omega, \tag{1a}$$

$$u = w \quad \text{on } \Gamma_{\mathrm{D}}, \tag{1b}$$

$$\mathrm{t}(\epsilon) = (\mathbb{C}\epsilon)|_{\Gamma}\vec{n} = g \quad \text{on } \Gamma_{\mathrm{N}}, \tag{1c}$$

$$u \cdot \vec{n} \leqslant 0, \quad \mathrm{t_n}(\epsilon) \leq 0, \quad (u \cdot \vec{n})\mathrm{t_n}(\epsilon) = 0, \quad \mathrm{t_t}(\epsilon) = 0 \quad \text{on } \Gamma_{\mathrm{C}}, \tag{1d}$$

where u is the displacement and $e = e(u) = \frac{1}{2}(\nabla u)^\top + \frac{1}{2}\nabla u$ the small-strain tensor, and $\mathbb{C}$ is the fourth order tensor of elastic moduli, while $\chi > 0$ a given relaxation time. Furthermore, $\vec{n} = \vec{n}(\vec{x})$ is the unit outward normal to $\Gamma = \partial\Omega$ at x, $\mathrm{t_n}(\epsilon) = \mathrm{t}(\epsilon) \cdot \vec{n}$, and $\mathrm{t_t}(\epsilon) = \mathrm{t}(\epsilon) - \mathrm{t_n}(\epsilon)\vec{n}$. It is straightforward to generalize the above problem formulation and all the results below to several (visco-)elastic solids in contact with a non-negative gap defined at a possible contact zone Γ_{C} (see Section 5.3). Actually, pertinent indications in this sense will be given at some places below. We further consider the initial-value problem for (1a)–(1d) for time $t > 0$ by prescribing the initial condition at $t = 0$

$$u(0) = u_0. \tag{1e}$$

The mechanical 1D analog of the above model is shown in Fig. 2. According to this figure, since the two components of the model are arranged in parallel, the strains in each component are identical and equal to $e(u)$, while for the stress it holds,

$$\sigma = \mathbb{C}e(u) + \chi\mathbb{C}e(\dot{u}), \tag{2}$$

where the actual (called also total) stress field is defined as the sum of the elastic and viscous part. The Kelvin–Voigt model is known to be very effective for predicting creep, but less at describing the relaxation behavior. For this reason other advanced and more complex rheological models exploiting auxiliary internal parameters have been defined and used. Eliminating these internal parameters leads to higher order time derivatives involved in the model, cf. Section 4.

3. Discretisation in time and space

We perform the discretisation of the initial-boundary value problem (1) by an implicit formula in time and by the BEM in space.

3.1. Time discretisation

Using an equidistant partition of the time interval $[0, T]$ with a time step $\tau > 0$ such that $T/\tau \in \mathbb{N}$, we consider:

$$\operatorname{div} \mathbb{C}\epsilon_\tau^k + f_\tau^k = 0 \quad \text{with } \epsilon_\tau^k = e\big(u_\tau^k + \chi(u_\tau^k - u_\tau^{k-1})/\tau\big) \quad \text{on } \Omega, \tag{3a}$$

$$u_\tau^k = w_\tau^k \quad \text{on } \Gamma_{\mathrm{D}}, \tag{3b}$$

$$\mathrm{t}(\epsilon_\tau^k) = \big(\mathbb{C}\epsilon_\tau^k\big)|_{\Gamma}\vec{n} = g_\tau^k \quad \text{on } \Gamma_{\mathrm{N}}, \tag{3c}$$

$$u_\tau^k \cdot \vec{n} \leqslant 0, \quad \mathrm{t_n}(\epsilon_\tau^k) \leq 0, \quad (u_\tau^k \cdot \vec{n})\mathrm{t_n}(\epsilon_\tau^k) = 0,$$
$$\mathrm{t_t}(\epsilon_\tau^k) = 0 \quad \text{on } \Gamma_{\mathrm{C}}, \tag{3d}$$

with $w_\tau^k = w(k\tau), f_\tau^k = f(k\tau)$ and $g_\tau^k = g(k\tau)$, and proceed recursively for $k = 1, \ldots, T/\tau$ with starting for $k = 1$ from

$$u_\tau^0 = u_0. \tag{3e}$$

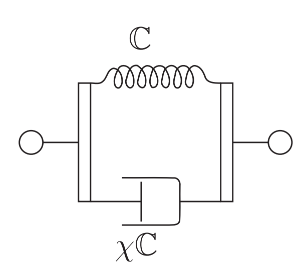

Fig. 2. Mechanical analog of the Kelvin–Voigt model.

This implicit time discretisation is numerically stable in the sense that the discrete solution u_τ^k stays bounded if $\tau \to 0$ in a suitable norm provided the data u_0, f, and g are qualified appropriately. More specifically, this can be seen from the discrete variant (as an upper inequality) of the continuous energy-conservation equality (30), introduced and discussed in Appendix, i.e.

$$\mathscr{E}(u_\tau^k) + \sum_{l=1}^{k} \int_\Omega \chi \mathbb{C} e\left(\frac{u_\tau^l - u_\tau^{l-1}}{\tau}\right) : e\left(\frac{u_\tau^l - u_\tau^{l-1}}{\tau}\right) \mathrm{d}x \leqslant \mathscr{E}(u_0) + \sum_{l=1}^{k}\left(\int_\Omega f_\tau^l \cdot \frac{u_\tau^l - u_\tau^{l-1}}{\tau} \mathrm{d}x + \int_{\Gamma_\mathrm{N}} g_\tau^l \cdot \frac{u_\tau^l - u_\tau^{l-1}}{\tau} \mathrm{d}S\right). \tag{4}$$

The inequality in (4) rely on convexity of the stored energy $\mathscr{E}$.

3.2. Transform of the visco-elastic to an auxiliary elastic-like problem

BEM standardly uses the so-called boundary integral operators which are explicitly known in specific static cases, here for the homogeneous linear elastic material which we consider in what follows. Yet, we have to calculate visco-elastic modification and here we benefit from choosing the ansatz of the tensor of viscous moduli as simply proportional to the elastic moduli, i.e. $\chi\mathbb{C}$. Therefore we can use the BEM with the same boundary integral operators as in the static case utilizing a transformation originally proposed in Roubíček (2013b) and numerically implemented in Roubíček et al. (2013), by defining a new auxiliary variable, in view of (1a), as

$$v_\tau^k = u_\tau^k + \chi \frac{u_\tau^k - u_\tau^{k-1}}{\tau}. \tag{5}$$

In terms of this new variable, one obviously has the Kelvin–Voigt strain $\epsilon_\tau^k = e(v_\tau^k)$, the velocity $(u_\tau^k - u_\tau^{k-1})/\tau = (v_\tau^k - u_\tau^{k-1})/(\tau + \chi)$, and the displacement recovered by

$$u_\tau^k = (\tau v_\tau^k + \chi u_\tau^{k-1})/(\tau + \chi), \tag{6}$$

which when used in (3a)–(3c), assuming $\Gamma_\mathrm{C} = \emptyset$, leads to the transformed time discretized problem

$$\operatorname{div} \mathbb{C} e(v_\tau^k) + f_\tau^k = 0 \quad \text{on } \Omega, \tag{7a}$$

$$v_\tau^k = \frac{\chi + \tau}{\tau} w_\tau^k - \frac{\chi}{\tau} w_\tau^{k-1} \quad \text{on } \Gamma_\mathrm{D}, \tag{7b}$$

$$\mathrm{t}(e(v_\tau^k)) = (\mathbb{C} e(v_\tau^k))|_\Gamma \vec{n} = g_\tau^k \quad \text{on } \Gamma_\mathrm{N}, \tag{7c}$$

with $u_\tau^{k-1} = (\tau v_\tau^{k-1} + \chi u_\tau^{k-2})/(\tau + \chi)$, and proceeding recursively for $k = 1, \ldots T/\tau \in \mathbb{N}$.

It might be easily observed from (7), that in terms of the auxiliary variable v_τ^k, which gives the equilibrium stress, the problem has the standard form of a linear elastic one and therefore could be numerically solved using any standard numerical procedure. However, BEM seems to be a natural choice, especially if we consider the case of zero body forces $f = 0$, which we adopt for the rest of this work.

What is actually computed by BEM is the auxiliary field v_τ^k, while we update the elastic field u_τ^k by (6), keeping in mind that u_τ^{k-1} is already known value at time step k. It is also important to notice that transformation (5) appears also in the boundary condition on Γ_D, see (7b), while tractions on Γ_N are equal to tractions in the original visco-elastic problem, as shown in (7c).

Taking into account the above explanation, the Somigliana displacement identity for the auxiliary variable v^k can be written as

$$C(\xi) v_\tau^k(\xi) + \int_\Gamma v_\tau^k(x) T(x,\xi) \,\mathrm{d}S_x = \int_\Gamma \mathrm{t}(e(v_\tau^k))(x) U(x,\xi) \,\mathrm{d}S_x, \tag{8}$$

where, the weakly and strongly singular integral kernels $U(x,\xi)$ and $T(x,\xi)$ are the usual Kelvin fundamental solutions in displacements and tractions (two-point tensor fields) (París and Cañas, 1997), $C(\xi)$ is the coefficient tensor of the free term (Mantič, 1993), and the first integral represents the Cauchy principal value.

3.3. Extension to multi-domain problems

In problems of several bodies, where some of them may be visco-elastic or merely elastic, we need to consider compatibility of displacements and equilibrium of tractions at common interfaces. Special attention is needed since, while we solve the BEM system with respect to the auxiliary field v_τ^k, compatibility of displacement has to be considered for the displacement field u_τ^k. Thus, at the interface between two visco-elastic solids Ω_1 and Ω_2 with relaxation times χ_1 and χ_2, respectively, the compatibility of displacements writes as

$$u_\tau^{k,1} = u_\tau^{k,2} \;\Rightarrow\; \frac{\tau}{\tau + \chi_1} v_\tau^{k,1} + \frac{\chi_1}{\tau + \chi_1} u_\tau^{k-1,1} = \frac{\tau}{\tau + \chi_2} v_\tau^{k,2} + \frac{\chi_2}{\tau + \chi_2} u_\tau^{k-1,2}, \tag{9}$$

where a variable $q_\tau^{k,i}$ refers to the domain Ω_i at the kth time step. For the case of elastic solids, where $\chi = 0$, Eq. (9) cast to the usual equation considered in a BEM formulation, that is $u_\tau^{k,1} = u_\tau^{k,2}$ reduces to $v_\tau^{k,1} = v_\tau^{k,2}$, as in this case the auxiliary field v_τ^k obviously coincides with the displacement field u_τ^k. Equilibrium of tractions is considered for the total stress field defined in (2) and consequently for the tractions t that correspond to the auxiliary field v_τ^k and these tractions are directly computed in the BEM formulation,

$$\mathrm{t}^1(e(v_\tau^k)) = -\mathrm{t}^2(e(v_\tau^k)). \tag{10}$$

3.4. Extension to contact problems utilizing the energetic approach in BEM

Visco-elastic frictionless contact problems are numerically handled usually by utilizing FEM, cf. (Chen et al., 1993; Barboteu et al., 2002, 2003; Fernández et al., 2003; Fernández and Sofonea, 2004; Mahmoud et al., 2007). To our best knowledge, except for the specific case of rolling contact (Kong and Wang, 1995), it is the first time that a BEM formulation for contact problems of visco-elastic solids is presented and fully explored, although it has been also used in Roubíček et al. (2013) and originally proposed in Roubíček (2013b). In order to solve the unilateral and/or adhesive contact problem of an assemblage of solids under (possible) contact to each other and/or some outer rigid obstacles, we can follow the general framework of energetic approaches to contact problems using BEM, as it is introduced in Panagiotopoulos et al. (2013a). Under this framework, the minimization of the potential energy, defined here in terms of the auxiliary variable v_τ^k from (5),

$$\mathscr{G}(k\tau, v_\tau^k) = \int_\Omega \frac{1}{2} \mathbb{C} e(v_\tau^k) : e(v_\tau^k) \mathrm{d}x - \int_{\Gamma_\mathrm{N}} g_\tau^k \cdot v_\tau^k \mathrm{d}S, \tag{11}$$

is required, assuming (7b). The same procedure has also been utilized in Roubíček et al. (2013), however without a detailed presentation and numerical testing of the BEM formulation for visco-elastic problems.

Here we assume a non-empty Γ_C and write the discretized condition (3d) in the form

$$v_\tau^k \cdot \vec{n} \leqslant -\frac{\chi}{\tau} u_\tau^{k-1} \cdot \vec{n}, \;\; \mathrm{t_n}(e(v_\tau^k)) \leq 0, \;\; \left(\left(v_\tau^k + \frac{\chi}{\tau} u_\tau^{k-1}\right) \cdot \vec{n}\right) \mathrm{t_n}(e(v_\tau^k)) = 0, \;\; \mathrm{t_t}(e(v_\tau^k)) = 0 \;\; \text{on } \Gamma_\mathrm{C}, \tag{12}$$

which completes the system of Eqs. (7). Following the energetic approach in BEM, we obtain a convex minimization problem in terms of the auxiliary field v_τ^k, in particular we have to solve the quadratic-programming problem:

$$\left.\begin{array}{lll}\text{minimize} & \mathscr{G}(k\tau, v_\tau^k) & \\ \text{subject to} & v_\tau^k\cdot\vec{n} \leqslant -\frac{\chi}{\tau}u_\tau^{k-1}\cdot\vec{n} & \text{on } \Gamma_\mathrm{C} \\ & v_\tau^k = \frac{\chi+\tau}{\tau}w_\tau^k - \frac{\chi}{\tau}w_\tau^{k-1} & \text{on } \Gamma_\mathrm{D}\end{array}\right\} \tag{13}$$

with $\mathscr{G}$ from (11).

Since the auxiliary variable v_τ^k gives the equilibrium stress, in contrast to the elastic field u_τ^k, the domain integral appearing in $\mathscr{G}$, under the assumption of zero body forces, can be expressed as a boundary one through the so-called Clapeyron theorem, i.e.

$$\int_\Omega \frac{1}{2}\mathbb{C}e(v_\tau^k) : e(v_\tau^k)\mathrm{d}x = \frac{1}{2}\int_\Gamma \mathfrak{t}(e(v_\tau^k))\cdot v_\tau^k \mathrm{d}x, \tag{14}$$

and finally the stored energy in terms of v_τ^k that we have to minimize, is given in the boundary form as

$$\mathscr{G}(k\tau, v_\tau^k) = \frac{1}{2}\int_\Gamma \mathfrak{t}(e(v_\tau^k))\cdot v_\tau^k\mathrm{d}x - \int_{\Gamma_\mathrm{N}} g_\tau^k\cdot v_\tau^k \mathrm{d}S. \tag{15}$$

Then, the standard techniques presented in Panagiotopoulos et al. (2013a) can be used to numerically handle the above minimization problem with $\mathscr{G}$ from (15) by utilizing BEM. It is worth mentioning that in the present implementation of this quadratic-programming problem only the part of the auxiliary field defined on Γ_C represents active variables in the minimization procedure (Panagiotopoulos et al., 2013a,b).

We sometimes are interested in visualizing the spatial distribution of the accumulated dissipated energy due to viscosity, that is the term $\int_0^t \chi\mathbb{C}e(\dot{u}) : e(\dot{u})\,\mathrm{d}t$ in (30). This is meaningful for the vast majority of visco-elastic problems, and not only for contact problems we study in this section. It is a standard procedure in BEM, that after solving the boundary value problem we compute displacements as well as stresses and strains in the whole domain by using the boundary values of displacements and tractions (París and Cañas, 1997). Having computed the stress and strain tensors in the required internal points for any time t_k, we may easily compute the above time integral for any time by using the previous time history. Similarly, the stored elastic energy can be computed at any time.

4. Other linear visco-elastic rheologies

The above method can be modified for other rheologies assuming again like in (2) that all the viscous and the elastic responses have the same tensorial character and thus are fully described just by only one tensor and several scalar constants. A generalized linear visco-elastic model, consisting of an assemblage of the Maxwell and Kelvin–Voigt elements together with free springs and dampers in series and/or parallel, might be represented by the following constitutive stress–strain relation in the form of a differential equation (Brinson and Brinson, 2010):

$$\sum_{k=0}^{n}\xi_k\frac{d^k\sigma}{dt^k} = \mathbb{C}e\left(\sum_{k=0}^{m}\chi_k\frac{d^ku}{dt^k}\right). \tag{16}$$

Obviously, certain restrictions on coefficients χ_k and ξ_k exist, see a detailed discussion in Flügge (1975).

Let us briefly present only a few special cases for which all the manipulation can lucidly be demonstrated and which simultaneously cover rheological models standardly used in most applications. Nevertheless, we could routinely continue for more complex rheologies with higher-order time derivatives on both sides, but the algebraic manipulation would become complicated and the requirement for an equal-tensorial character more restrictive. For simplicity, in this section we do not consider the unilateral contact, i.e. $\Gamma_\mathrm{C} = \emptyset$, and, like before, we neglect inertial and external bulk forces. We further restrict ourselves, for implementation and notational purposes, to the case of the second-order stress–strain relation in (16), i.e. $n = m = 2$, which is given in the following form:

$$\xi_2\ddot{\sigma} + \xi_1\dot{\sigma} + \xi_0\sigma = \mathbb{C}e(\chi_2\ddot{u} + \chi_1\dot{u} + \chi_0 u), \tag{17}$$

requiring some initial conditions for displacements and stresses and their time derivatives of at most of the first order, depending on the values of parameters χ_k and ξ_k. The general form of equations that governs the system is,

$$\mathrm{div}\,\sigma = 0 \quad \text{on } \Omega, \tag{18a}$$

$$u = w \quad \text{on } \Gamma_\mathrm{D}, \tag{18b}$$

$$\sigma\vec{n} = g \quad \text{on } \Gamma_\mathrm{N}. \tag{18c}$$

The implicit time discretisation of Eq. (17) assuming a fixed time step τ, leads to

$$\begin{aligned}&\xi_2\frac{\sigma_\tau^k - 2\sigma_\tau^{k-1} + \sigma_\tau^{k-2}}{\tau^2} + \xi_1\frac{\sigma_\tau^k - \sigma_\tau^{k-1}}{\tau} + \xi_0\sigma_\tau^k \\ &\quad = \mathbb{C}e\left(\chi_2\frac{u_\tau^k - 2u_\tau^{k-1} + u_\tau^{k-2}}{\tau^2} + \chi_1\frac{u_\tau^k - u_\tau^{k-1}}{\tau} + \chi_0 u_\tau^k\right)\end{aligned} \tag{19}$$

and, after an elementary algebra, the time-discrete variant of (17) and (18) reads as

$$\begin{aligned}\mathrm{div}\,\sigma_\tau^k = 0 \quad \text{with } \sigma_\tau^k = \mathbb{C}e\bigg(&\frac{\chi_2 + \tau\chi_1 + \chi_0\tau^2}{\xi_2 + \tau\xi_1 + \xi_0\tau^2}u_\tau^k - \frac{2\chi_2 + \tau\chi_1}{\xi_2 + \tau\xi_1 + \xi_0\tau^2}u_\tau^{k-1} \\ &+ \frac{\chi_2}{\xi_2 + \tau\xi_1 + \xi_0\tau^2}u_\tau^{k-2}\bigg) + \frac{2\xi_2 + \tau\xi_1}{\xi_2 + \tau\xi_1 + \xi_0\tau^2}\sigma_\tau^{k-1} \\ &- \frac{\xi_2}{\xi_2 + \tau\xi_1 + \xi_0\tau^2}\sigma_\tau^{k-2} \quad \text{on } \Omega,\end{aligned} \tag{20}$$

completed by the boundary conditions $u_\tau^k = w_\tau^k$ on Γ_D and $\sigma_\tau^k\vec{n} = g_\tau^k$ on Γ_N.

The implementation of BEM relies on $\mathrm{div}\,\sigma_\tau^{k-1} = 0$ and $\mathrm{div}\,\sigma_\tau^{k-2} = 0$, and furthermore, likewise in (5), on the definition of an auxiliary field of the general form

$$\begin{aligned}v_\tau^k = &\frac{\chi_2 + \tau\chi_1 + \chi_0\tau^2}{\xi_2 + \tau\xi_1 + \xi_0\tau^2}u_\tau^k - \frac{2\chi_2 + \tau\chi_1}{\xi_2 + \tau\xi_1 + \xi_0\tau^2}u_\tau^{k-1} \\ &+ \frac{\chi_2}{\xi_2 + \tau\xi_1 + \xi_0\tau^2}u_\tau^{k-2},\end{aligned} \tag{21}$$

giving

$$\begin{aligned}\sigma_\tau^k = \mathbb{C}e(v_\tau^k) &+ \frac{2\xi_2 + \tau\xi_1}{\xi_2 + \tau\xi_1 + \xi_0\tau^2}\sigma_\tau^{k-1} \\ &- \frac{\xi_2}{\xi_2 + \tau\xi_1 + \xi_0\tau^2}\sigma_\tau^{k-2} \quad \text{on } \Omega.\end{aligned} \tag{22}$$

The transformed system of equations that we actually solve using BEM has the form

$$\mathrm{div}\,\mathbb{C}e(v_\tau^k) = 0 \quad \text{on } \Omega, \tag{23a}$$

$$\begin{aligned}v_\tau^k = &\frac{\chi_2 + \tau\chi_1 + \chi_0\tau^2}{\xi_2 + \tau\xi_1 + \xi_0\tau^2}w_\tau^k - \frac{2\chi_2 + \tau\chi_1}{\xi_2 + \tau\xi_1 + \xi_0\tau^2}w_\tau^{k-1} \\ &+ \frac{\chi_2}{\xi_2 + \tau\xi_1 + \xi_0\tau^2}w_\tau^{k-2} \quad \text{on } \Gamma_\mathrm{D},\end{aligned} \tag{23b}$$

$$\begin{aligned}\mathfrak{t}(e(v_\tau^k)) = \left(\mathbb{C}e(v_\tau^k)\right)|_\Gamma\vec{n} = g_\tau^k &- \frac{2\xi_2 + \xi_1\tau}{\xi_2 + \xi_1\tau + \xi_0\tau^2}g_\tau^{k-1} \\ &+ \frac{\xi_2}{\xi_2 + \xi_1\tau + \xi_0\tau^2}g_\tau^{k-2} \quad \text{on } \Gamma_\mathrm{N}.\end{aligned} \tag{23c}$$

Solving the above system with BEM we obtain the pair v_τ^k and $\mathfrak{t}(e(v_\tau^k))$, for each time step k. Then, we may also compute σ_τ^k, by evaluating $\mathbb{C}e(v_\tau^k)$ in Ω by standard BIR (París and Cañas, 1997) and adding σ^{k-1} and σ^{k-2} according to (22). The reconstruction of the physical displacement field is carried out by solving Eq. (21) for u_τ^k,

$$u_\tau^k = \frac{\xi_2 + \tau\xi_1 + \xi_0\tau^2}{\chi_2 + \tau\chi_1 + \chi_0\tau^2} v_\tau^k + \frac{2\chi_2 + \tau\chi_1}{\chi_2 + \tau\chi_1 + \chi_0\tau^2} u_\tau^{k-1} - \frac{\chi_2}{\chi_2 + \tau\chi_1 + \chi_0\tau^2} u_\tau^{k-2}, \tag{24}$$

and, following (22), the total traction (physical traction) field $p_\tau^k = \sigma_\tau^k \vec{n}$ is reconstructed by

$$p_\tau^k = \mathfrak{t}(e(v_\tau^k)) + \frac{2\xi_2 + \xi_1\tau}{\xi_2 + \xi_1\tau + \xi_0\tau^2} p_\tau^{k-1} - \frac{\xi_2}{\xi_2 + \xi_1\tau + \xi_0\tau^2} p_\tau^{k-2}. \tag{25}$$

All the necessary initial values, appearing above for discrete time lower than zero, are assumed to be equal to zero. Calculation of characteristic physical parameters is just a post-processing procedure and depends on each specific model. E.g., elastic stresses of the Kelvin–Voigt model can be obtained recursively by applying the elastic stress operator $\mathbb{C}e(\cdot)$ to (6), which is a particularization of (24). Some of the models that could be represented by the second order differential equation (17) are listed in Table 1; see also (Brinson and Brinson, 2010). It is worth mentioning that the system of equations (23) could obviously be solved by any other appropriate numerical method (e.g., FEM as in Mesquita et al. (2001)), and that more complicated visco-elastic models of a higher-order, i.e. $m > 2$ or $n > 2$ in (16), could be accomplished within the current framework with the only difference that higher order derivatives will appear.

Within the class of constitutive relations defined by (17), we will consider several selected rheologies shown in Table 1. The discrete energy estimates like (4) can be derived for each of them after suitable, sometimes rather complicated manipulation (not performed in this article, however).

Table 1
Some models that could be represented by the constitutive differential Eq. (17) with pertinent coefficients χ_k and ξ_k, present ($\neq 0$) indicated by ✓ or absent ($= 0$) by ×.

Model	Name	χ_0	χ_1	χ_2	ξ_0	ξ_1	ξ_2
	Elastic (Hooke) solid	✓	×	×	✓	×	×
	Viscous (Newton) fluid	×	✓	×	✓	×	×
	Maxwell fluid	×	✓	×	✓	✓	×
	Kelvin-Voigt solid	✓	✓	×	✓	×	×
	Boltzmann or Standard linear or 3-parameter solid	✓	✓	×	✓	✓	×
	Jeffreys or 3-parameter fluid	×	✓	✓	✓	✓	×
	Burgers or 4-parameter fluid	×	✓	✓	✓	✓	✓
	4-parameter solid	✓	✓	✓	✓	✓	×

5. Numerical examples

The above introduced framework has been implemented in an open BEM Java code (Panagiotopoulos, 2009) with capabilities of 2D and 3D elastostatic analysis, among others. This code is supplied with all the necessary "modules" for the energetic approach in BEM used for contact problems, and has also been employed in several related works of the authors (Roubíček et al., 2013; Panagiotopoulos et al., 2013a,b).

5.1. Visco-elastic creep behavior

This first example might be seen as a "benchmark", since it is one of the most frequent examples met in the literature in order to compare numerical to analytical solutions of visco-elasticity (e.g. in Mesquita and Coda (2002)).

Fig. 3 depicts the geometry and boundary conditions of the problem together with a physical interpretation of the visco-elastic material. The physical properties and the geometry of the problem are given in Table 2, where for the first variant of the problem we assume a Kelvin–Voigt material with viscosity μ_1, without the spring $\alpha\mathbb{C}$ and the damper $\mu_2\mathbb{C}$ depicted in Fig. 3. The uniform BEM mesh for this problem has 180 linear elements. Two time steps have been used, a coarse and a fine one, $\tau_c = 10$ (days) and $\tau_f = 1$ (day) respectively, in order to observe numerically the accuracy of the time integration scheme. Prescribed tractions, applied on the right-hand side of the domain for $0 < t \leq t_r$, have normal and tangential components $p_n = 5$ (N/mm^2) and $p_t = 0$, respectively. The total time of analysis is $T = 800$ (days). The external loading is removed at time $t_r = 400$ (days), i.e. after this time $p_n = 0$.

Computed displacements are plotted in time in Fig. 4 together with the analytic solution, which can be easily deduced for this simple problem. Both numerical solutions for a coarse and a fine time step, are plotted. Notice that the fine-time-step solution is not shown in the plot for all time steps but only for those of the coarse partition of the time interval. An excellent agreement of the fine-time-step solution with the analytic one is observed, the coarse-time-step solution being also very good. Fig. 5 shows the evolution in time of the total stresses at the geometric center of the solid. Recall that for the present case of the Kelvin–Voigt model, the *total stress field*, $\sigma_\tau^k = \mathbb{C}e(v_\tau^k)$, corresponds directly to the auxiliary field v_τ^k, while the *elastic stress field*, $\mathbb{C}e(u_\tau^k)$, corresponds to the u_τ^k field. Then, the *viscous stresses* can be computed as the difference of the total minus elastic stresses.

Table 2
Viscoelastic and geometrical properties of the models used in examples of Section 5.1.

L (mm)	800
h (mm)	100
μ_1 (days)	45.454545
E (kN/mm^2)	11
ν	0.0

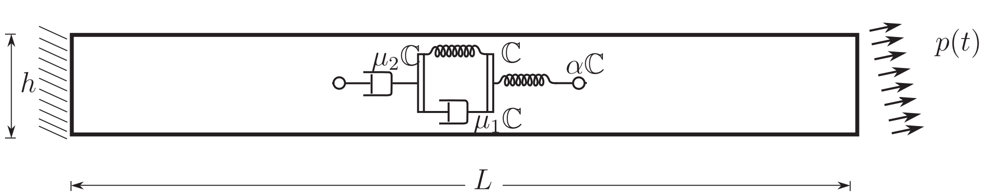

Fig. 3. Geometry of the problem and physical interpretation.

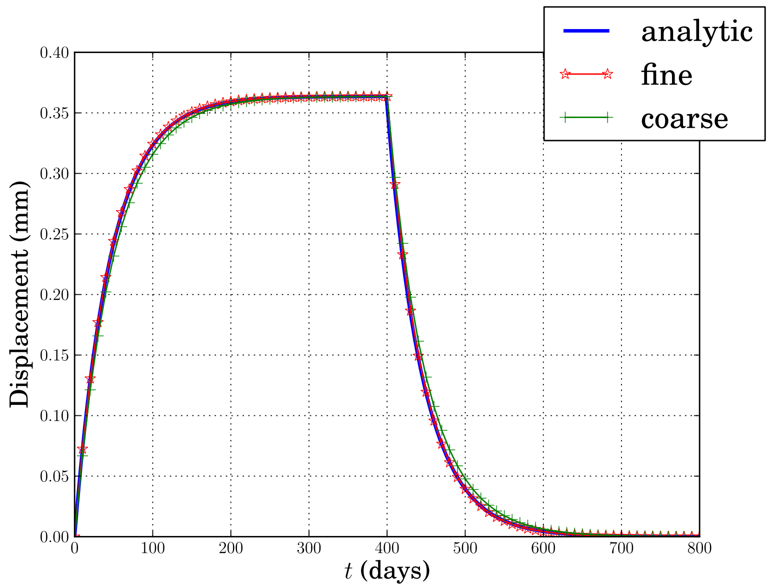

Fig. 4. Displacement for the Kelvin–Voigt material, fine time partition solution shown here with one time point per ten steps.

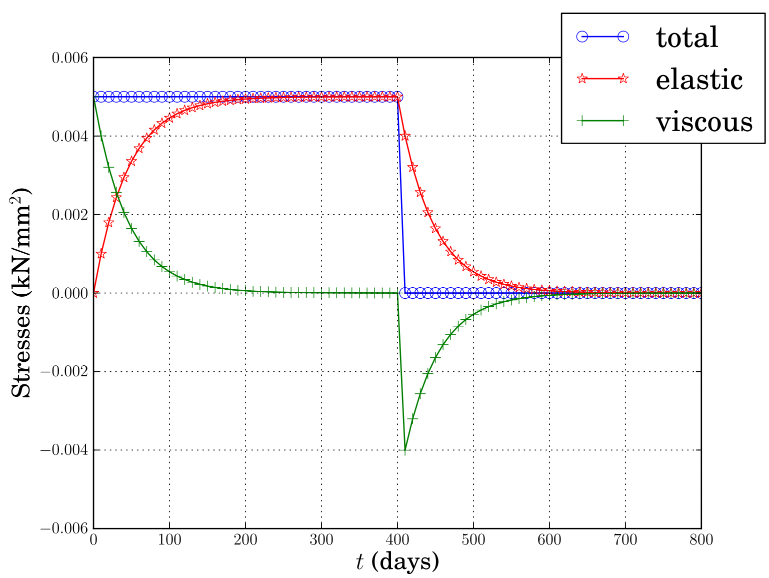

Fig. 5. Stress σ_{xx}, for the Kelvin–Voigt material, at the centroid of the solid with one time point shown per ten steps, which means that only 80 time points are plotted, instead of 800 that actually have been calculated.

In the second variant of this problem, the prescribed tractions on the right-hand side have components $p_n = 0$ and $p_t = 5$ (N/mm^2), with the loading applied from the time $t_i = 80$ (days) to $t_r = 533.33$ (days), while $T = 800$ (days). Numerical results are obtained using time step τ=1 (day). In this case we show the spatial distribution of the dissipated energy density due to the viscosity over the time interval $[0, T]$ for the Kelvin–Voigt model, and compare the kinematic response of several visco-elastic rheologies presented in this article.

Fig. 6 shows the BEM mesh (used for both variants of the problem) together with a deformed configuration for the case of vertical loading. In Fig. 7 the spatial distribution of the dissipated energy density $\int_0^T \chi \mathbb{C} e(\dot{u}) : e(\dot{u})\,\mathrm{d}t$, in (J/m^2), is visualized. It can be observed there, that the main part of the dissipated energy is accumulated, during the evolution in time, in a region close to the left fixed side of the solid where the highest normal stresses σ_{xx} can be expected.

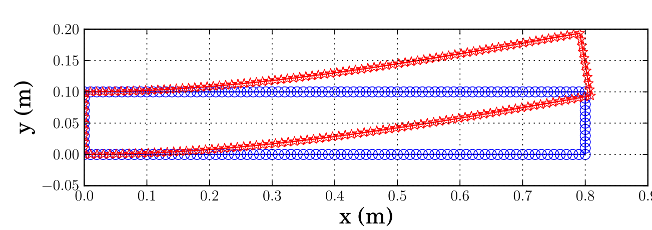

Fig. 6. Deformed configuration, for the Kelvin–Voigt material, for the case of vertical loading, at time $t = T/2$.

For the other visco-elastic models studied we use the parameter values $\alpha = 2, \mu_2 = \mu_1$, where their nonzero values are required. For example, we may assume existence of the damper μ_2 and the spring of stiffness $\mathbb{C}$, with simultaneous absence of the other two components, in order to simulate the Maxwell model. The results

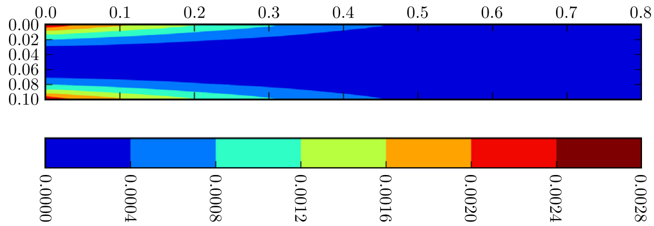

Fig. 7. Spatial distribution of the dissipated energy density $\int_0^T \chi \mathbb{C} e(\dot{u}) : e(\dot{u})\,\mathrm{d}t$, in (J/m^2), for the case of vertical loading and the Kelvin–Voigt material.

are shown in Fig. 8, where models have been divided into two categories: (a) solid-type and (b) fluid-type, because of different order of response values. It might be observed in this figure the ability of the algorithm to compute a jump in displacement due to a jump of forces for the case of both the Hooke and Boltzmann models in contrast to the Kelvin–Voigt model, where a smoother increase of displacement takes place.

5.2. 3D analysis of an ellipsoidal cavity embedded in an infinite medium

This example shows the capabilities of the procedure developed and implemented also for 3D visco-elastic problems, see (Schanz et al., 2005; Guo and Peng, 1991), for other 3D BEM implementations. The problem of an ellipsoidal cavity in a visco-elastic medium under remote stress field is solved. The Kelvin–Voigt material considered has Young's modulus $E = 70$ (GPa), Poisson's ratio $\nu = 0.35$ and relaxation time $\chi = 45.454545$ (days). The remote stress field is applied on a cube with side length $L = 36$ (m) representing an infinite visco-elastic medium with an embedded ellipsoidal cavity placed in its center. The geometry of the ellipsoid is defined in Cartesian coordinates by the equation

$$\frac{x^2}{a^2} + \frac{y^2}{b^2} + \frac{z^2}{c^2} = 1, \tag{26}$$

with $a = 0.8$ (m), $b = 0.9$ (m) and $c = 1$ (m). The BEM mesh of the ellipsoid consists of 264 four node isoparametric quadrilateral elements, while the cube boundary is discretised by 96 elements, see Fig. 9. Uniform normal tractions $\sigma_x = 25$ (GPa), $\sigma_y = 25$ (GPa) and $\sigma_z = 100$ (GPa) are applied on the cube faces perpendicular to the x-, y- and z-axis, respectively. The cavity boundary is free. The time pattern of the load has three parts: initially the load increases linearly with time, then it is constant in time, and finally it jumps down to zero, as can be seen in Fig. 10. As only Neumann boundary conditions are prescribed, to avoid rigid body motions we apply the *F1 method* of Blázquez et al. (1996); to the best of our knowledge, first time implemented in the 3D case.

5.3. Visco-elastic solid in contact

A problem including frictionless contact between a viscoelastic solid and a rigid obstacle is solved by the BEM, to the best of our knowledge, for the first time. The Kelvin–Voigt rheology is assumed. In particular, the indentation of a half disk against a rigid foundation is considered under plane strain conditions. In this advancing contact problem the length of the contact zone depends on the load value. The problem geometry is shown in Fig. 11. The radius of the disk is $r = 0.75$ m. The potential contact zone is defined

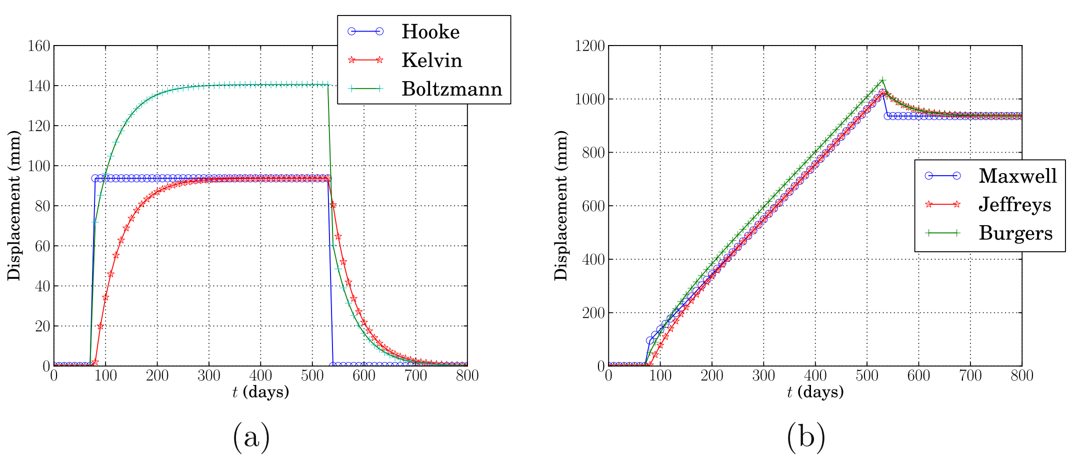

Fig. 8. Vertical displacement of the right-hand edge computed by six different rheology models, distinguished as (a) solid-type and (b) fluid-type.

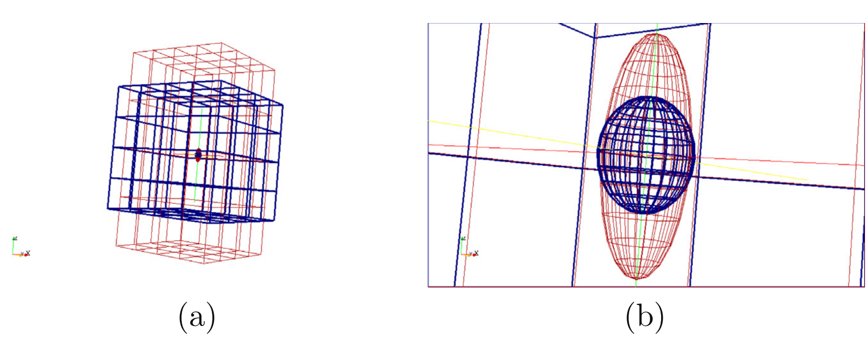

Fig. 9. (a) Undeformed and deformed BEM mesh of cube with the embedded ellipsoidal cavity, shown in detail in (b), at time $t = 400$ (sec). Scale factor of 500 is used to magnify displacements.

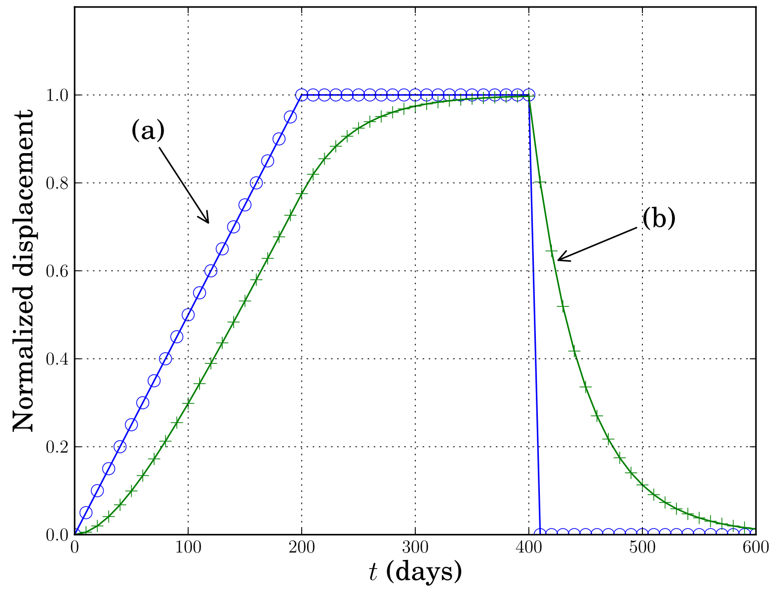

Fig. 10. Time evolution of the displacement of the positive Z pole of ellipsoid, normalized by the maximum value of this displacement in the elastic case ($u_e^{max} = 2.224$ mm). (a) Elastic material, (b) Visco-elastic Kelvin–Voigt material (the maximum value of this displacement is $u_v^{max} = 2.218$ mm). The time evolution pattern of the external loading coincides with the displacement evolution in the elastic case.

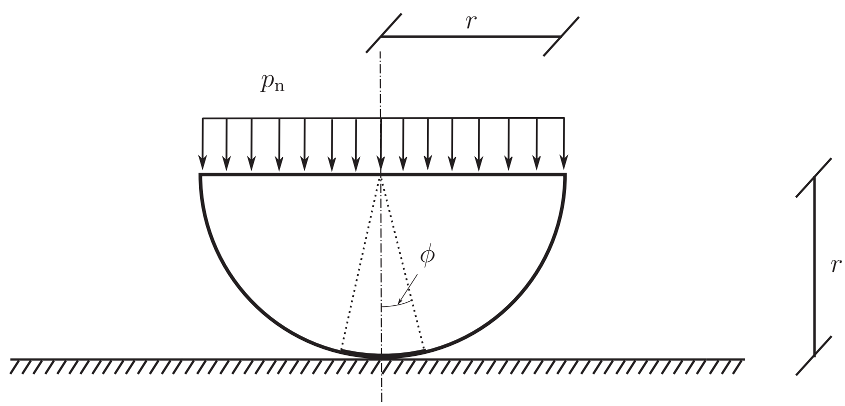

Fig. 11. A visco-elastic half disk pressed against the rigid foundation.

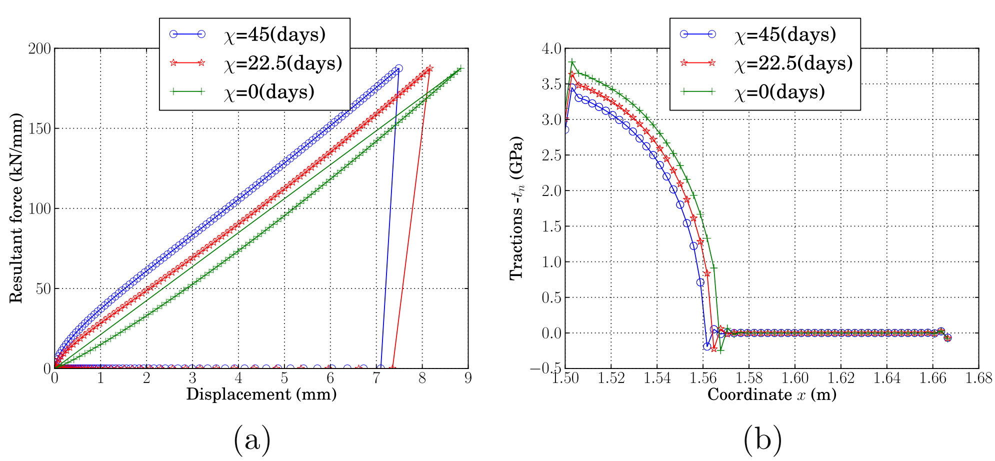

Fig. 12. (a) Total resultant vertical force on the horizontal side of the half disk versus the absolute value of the vertical displacement of the central point of this side. (b) Normal elastic tractions along the possible contact zone at the time of peak loading t_p.

by the angle $\phi = 13.5(°)$. Normal tractions are increased linearly in time from zero to $p_n = -250$ (GPa) at time $t_p = 250$ (days) and then they are removed. We study the response up to the total time $T = 500$ (days). Tangential tractions along the whole straight edge of the half disk are zero. Due to the problem symmetry only the quarter disc is modeled. The Kelvin–Voigt material has Young's

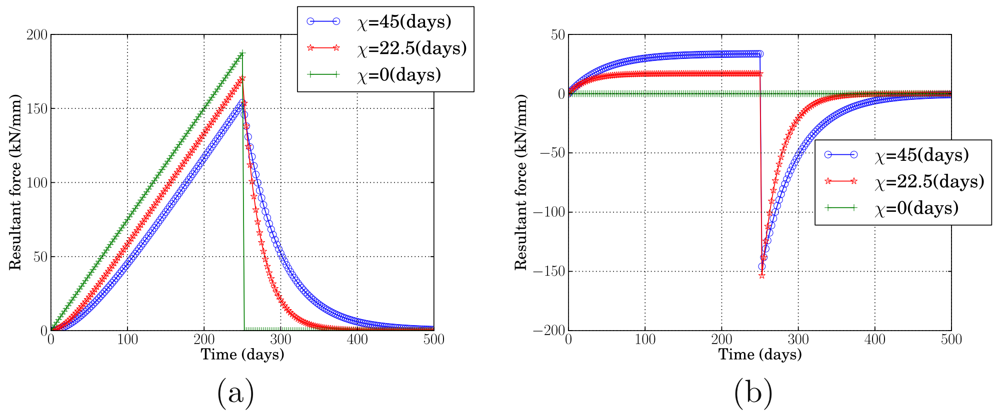

Fig. 13. (a) Elastic resultant force with time. (b) Viscous resultant force with time.

modulus $E = 70$ (GPa) and Poisson's ratio $\nu = 0.35$. For comparison purposes, three relaxation times are considered: $\chi = 0$, 22.5 (days) and 45 (days).

The numerical solution of this problem, which includes the determination of the contact zone, is accomplished as described in Section 3.4, through the minimization of the potential energy. The BEM mesh of the quarter disk consists of 270 linear elements with 60 elements along the possible contact zone defined by the angle ϕ, 170 elements for the rest of the circular curve and 20 elements for each one of the two straight lines. The time step of $\tau = 2.5$ (days) is used, for the three relaxation times considered, resulting in 200 time steps.

The advancing contact problem is non-linear and this can be verified from Fig. 12(a), where for the non-viscous case and after the loading is removed the solution directly returns to the initial configuration. It might be seen there, that the straight line that connects the "peak" loading point back to the initial configuration is different from the non-linear path computed from the initial undeformed configuration to the peak point. The behavior of the visco-elastic cases is different, where we observe that the greater the viscosity the greater the difference from the elastic case. For the viscous cases, we notice that after the loading vanishes at the time t_p, the total force jumps to zero as well, while elastic and viscous forces of opposite signs still remain and vanish progressively. It is also easily verified from Fig. 12(b) that the length of the contact zone depends on χ value. It can been observed there that the greater the viscosity, lower the length of the contact zone and lower the maximum absolute value of the normal elastic tractions. This last observation may also be noticed in Fig. 13(a), where the evolution in time of the elastic part of the resultant force is plotted for all three viscosity cases. Finally, in Fig. 13(b) the evolution of the viscous part of the resultant force is plotted, where it is interesting to observe a jump and a finite peak in these viscous forces at the time of the loading removal t_p for $\chi > 0$.

6. Conclusions

In this paper, an advanced formulation for the solution of quasi-static linear visco-elastic problems for a broad spectrum of rheologies, which further develops the original proposal by Mesquita, Coda and co-workers (Mesquita et al., 2001; Mesquita and Coda, 2002), has been presented. The resulting problem can be solved using standard numerical methods such as FEM and BEM.

We have confined ourselves to materials responding on the mechanical loading in such a way that, roughly speaking, the tensorial and the rheological features are separated; this means only one tensor is used to describe all the elastic and viscous processes which then are distinguished only be scalar constants. Since, we have been able to cast the problem using boundary formulas only, the BEM appears as the most reasonable method to solve both 2D and 3D problems. After a certain "computationally cheap" algebraic manipulation, only the standard Kelvin's fundamental solution of elasticity is required for the BEM implementation. Furthermore, an extension and implementation to contact problems of visco-elastic continua is presented as well.

Using this formulation, the well known Kelvin–Voigt model has been scrutinized and it has been shown that several other, more complex models, can be confronted. A quite detailed presentation has been given for several models using the Maxwell, Boltzmann, Jeffreys and Burgers rheologies.

Incorporation of this framework to existing BEM codes is very easy, at least for problems of visco-elasticity, since just a transformed auxiliary field has to be defined. After solving the problem for this auxiliary field, the actual stresses and displacements can be easily reconstructed. For unilateral contact problems, further features of the energetic approach in BEM are needed. Numerical solutions of problems presented in this paper are accomplished by an in-house open BEM code, implemented in Java.

Some standard problems of 2D and 3D visco-elasticity as well as a problem of contact mechanics have been numerical solved and analyzed in order to validate the suitability of the methodology developed for solving realistic visco-elasticity problems.

An extension of the current framework to problems of adhesive contact or also to more complex problems, where interface damage and/or interface plasticity are taken into account, is possible and into some extent has already been accomplished in other concurrent works of the authors (e.g. Roubíček et al., 2013; Kružík et al., 2014).

Acknowledgments

The authors thank to two anonymous reviewers for their constructive comments, which were helpful in improving the manuscript. The authors acknowledge the support by the Junta de Andalucía and Fondo Social Europeo (Proyecto de Excelencia TEP-4051), by the Ministerio de Economía y Competitividad (Proyecto MAT2012-37387), as well as from the Grants 201/09/0917, 201/10/0357, and 13-18652S (GA ČR) together with the institutional support RVO: 61388998 (ČR).

Appendix: The energetics of selected rheological models

All rheological models above allow for clear energetic balance, which is important in many respects. We will illustrate it only for the standard linear solid and, as special cases, for the Maxwell and the Kelvin–Voigt models, i.e. (16) for $m \leq 1$ and $n \leq 1$.

The energetics for the standard linear solid (and for Maxwell material too) needs an introduction of one *internal variable* with the meaning of a strain, let us denote it by π, acting in an additive decomposition of the total strain $e(u)$, i.e.

$$e(u) = e_{\mathrm{el}} + \pi. \tag{27}$$

The elastic strain e_{el} occurs on the "serial" elastic spring (let us denote its elastic-moduli tensor by $\mathbb{C}_{\mathrm{M}}$) while π occurs on the "parallel" elastic spring (with the elastic moduli $\mathbb{C}_{\mathrm{KV}}$) and on the damper (with the viscous moduli tensor $\mathbb{D}$), cf. the 5th row in Table 1. The *stored energy* is then

$$E(e_{\mathrm{el}}, \pi) = \int_\Omega \left(\frac{1}{2}\mathbb{C}_{\mathrm{M}} e_{\mathrm{el}} : e_{\mathrm{el}} + \frac{1}{2}\mathbb{C}_{\mathrm{KV}}\pi : \pi\right)\mathrm{d}x \tag{28}$$

while the dissipation rate is $\mathbb{D}\dot{\pi} : \dot{\pi}$. Abbreviating $\mathscr{E}(u,\pi) = E(e(u)-\pi, \pi)$, testing (18a) by $\dot{u}$ and using the rheological ansatz (16) and the boundary conditions (18b), (18c), after a little calculus one obtains the *total energy balance* in the form:

$$\begin{aligned}&\mathscr{E}(u(t),\pi(t)) + \int_0^t \int_\Omega \mathbb{D}\dot{\pi} : \dot{\pi}\,\mathrm{d}x\mathrm{d}t\\ &\quad = \mathscr{E}(u_0,\pi_0) + \int_0^t \left(\int_\Omega f\cdot\dot{u}\,\mathrm{d}x + \int_{\Gamma_{\mathrm{N}}} g\cdot\dot{u}\,\mathrm{d}S\right)\mathrm{d}t.\end{aligned} \tag{29}$$

For simplicity, here we assumed homogeneous Dirichlet condition $w = 0$. The time integrals on the left- and right-hand side of (29) represent the dissipated energy due to viscosity and the work of external forces done over the time interval $[0,t]$, respectively. Note that we need to prescribe the initial conditions both $u(0,\cdot) = u_0$ and $\pi(0,\cdot) = \pi_0$. In a general case if $w \neq 0$, one can first make a substitution of $u - \bar{w}$ with an extension $\bar{w}$ of the boundary data w inside the bulk domain and then formulate an energy balance for a "shifted" solution satisfying homogeneous Dirichlet condition but with a modified loading f and g while the internal variable π remains unaffected.

As a special case, we can get both the Kelvin–Voigt model and the Maxwell model. The former model results as the limit for $\mathbb{C}_{\mathrm{M}} \to \infty$, which yields $e_{\mathrm{el}} = 0$ so that simply $e(u) = \pi$ and, for $\mathbb{D} = \chi\mathbb{C}$, the energy balance (29) simplifies as

$$\begin{aligned}&\mathscr{E}(u(t)) + \int_0^t \int_\Omega \chi\mathbb{C}e(\dot{u}) : e(\dot{u})\,\mathrm{d}x\mathrm{d}t\\ &\quad = \mathscr{E}(u_0) + \int_0^t \left(\int_\Omega f\cdot\dot{u}\,\mathrm{d}x + \int_{\Gamma_{\mathrm{N}}} g\cdot\dot{u}\mathrm{d}S\right)\mathrm{d}t,\end{aligned} \tag{30}$$

with $\mathscr{E}(u) = \int_\Omega \frac{1}{2}\mathbb{C}e(u) : e(u)\mathrm{d}x$. The Maxwell model results as the limit for $\mathbb{C}_{\mathrm{KV}} \to 0$; the splitting (27) and in particular the internal variable π remains in this model.

The other higher-order models need more involved considerations and we will not present it here. In particular, the 4-parameter solid uses again (27) but the Burgers rheology, having two "free nodes" (cf. the rheological scheme at the 7th row in Table 1), needs introduction of two internal variables and decomposition of $e(u)$ in (27) into 3 terms.

Under appropriate qualification of the external loading and the initial conditions, energy balance (30) gives also a priori estimates of the solutions in respective norms by using typically the Gronwall, the Young, and the Hölder inequalities. Due to convexity of the energy $\mathscr{E}(\cdot)$, this manipulation can be reflected to the implicit time-discretisation schemes considered in this paper, yielding numerical stability and convergence of such schemes for $\tau \to 0$. In our linear situation, this convergence is indeed simple.

Evaluation and visualization of the spatial distribution of the energies occurring in balances like (29) or (30) may be of a special interest, since it shows in which regions of the body the dissipation takes place, see the numerical example of Section 5.1 or Roubíček et al. (2013). This energy dissipation leads to a heat production (not considered here, however), and thus its spatial distribution would be important when solving the heat-transfer problem in a possibly full thermomechanical coupling. These forms of energetics are also of interest, since they could be used to solve contact problems of visco-elastic bodies, see Section 5.3, or even more complex problems where also inelastic phenomena take place on the boundaries (or interfaces) of the viscous bodies, cf. (Roubíček et al., 2013). Techniques for the evaluation of these energies in combination with BEM have been briefly described in Sections 3.4 and 4, and employed in Section 5.

References

Barboteu, M., Han, W., Sofonea, M., 2002. A frictionless contact problem for viscoelastic materials. J. Appl. Math. 2, 1–21.

Barboteu, M., Hoarau-Mantel, T.V., Sofonea, M., 2003. On the frictionless unilateral contact of two viscoelastic bodies. J. Appl. Math. 11, 575–603.

Blázquez, A., Mantič, V., París, F., Cañas, J., 1996. On the removal of rigid body motion in the solution of elastostatic problems by direct BEM. Int. J. Numer. Methods Eng. 39, 4021–4038.

Brinson, H.F., Brinson, L.C., 2010. Polymer Engineering Science and Viscoelasticity: An Introduction. Springer, New York.

Carini, A., Gioda, G., 1986. A boundary integral equation technique for visco-elastic stress analysis. Int. J. Numer. Anal. Methods Geomech. 10, 585–608.

Cezario, F., Santiago, J.A.F., Oliveira, R.F., 2011. Two-dimensional version of Sternberg and Al-Khozaie fundamental solution for viscoelastic analysis using the boundary element method. Eng. Anal. Boundary Elem. 35, 836–844.

Chen, Y.C., Hwu, C., 2011. Boundary element analysis for viscoelastic solids containing interfaces/holes/cracks/inclusions. Eng. Anal. Boundary Elem. 35, 1010–1018.

Chen, W.H., Chang, C.M., Yeh, J.T., 1993. An incremental relaxation finite element analysis of viscoelastic problems with contact and friction. Comput. Methods Appl. Mech. Eng. 109, 315–329.

Fernández, J.R., Sofonea, M., 2004. Numerical analysis of a frictionless viscoelastic contact problem with normal damped response. Comput. Math. Appl. 47, 549–568.

Fernández, J.R., Han, W., Sofonea, M., 2003. Numerical simulations in the study of frictionless contact problems. Int. J. Appl. Math. Comput. Sci. 30, 97–105.

Flügge, W., 1975. Viscoelasticity, second ed. Springer-Verlag, New York.

Graham, G.A.C., 1965. The contact problem in the linear theory of viscoelasticity. Int. J. Eng. Sci. 3, 27–46.

Guo, L.B., Peng, S.S., 1991. A three-dimensional boundary element method for piecewise homogeneous viscoelastic media and its application in mining engineering. Min. Sci. Technol. 12, 241–251.

Huang, Y., Crouch, S.L., Mogilevskaya, S.G., 2005a. A time domain direct boundary integral method for a viscoelastic plane with circular holes and elastic inclusions. Eng. Anal. Boundary Elem. 29, 725–737.

Huang, Y., Crouch, S.L., Mogilevskaya, S.G., 2005b. Direct boundary integral procedure for a Boltzmann viscoelastic plane with circular holes and elastic inclusions. Comput. Mech. 37, 110–118.

Kong, X.A., Wang, Q., 1995. A boundary element approach for rolling contact of viscoelastic bodies with friction. Comput. Struct. 54, 405–413.

Kružík, M., Panagiotopoulos, C.G., Roubíček, T., 2014. Quasistatic adhesive contact delaminating in mixed mode and its numerical treatment. Math. Mech. Solids (in print) http://dx.doi.org/10.1177/1081286513507942.

Kusama, T., Mitsui, Y., 1982. Boundary element method applied to linear viscoelastic analysis. Appl. Math. Model. 6, 285–290.

Lee, S.S., Westmann, R.A., 1995. Application of high-order quadrature rules to time-domain boundary element analysis of viscoelasticity. Int. J. Numer. Methods Eng. 38, 607–629.

Mahmoud, F.F., El-Shafei, A.G., Mohamed, A.A., 2007. An incremental adaptive procedure for viscoelastic contact problems. ASME J. Tribol. 129, 305–313.

Manolis, G.D., Beskos, D.E., 1981. Dynamic stress concentration studies by boundary integrals and Laplace transforms. Int. J. Numer. Methods Eng. 17, 573–599.

Mantič, V., 1993. A new formula for the C-matrix in the Somigliana identity. J. Elast. 33, 191–201.

Marques, S.P.C., Creus, G.J., 2012. Computational Viscoelasticity. Springer, New York.

Mesquita, A.D., Coda, H.B., 2002. Boundary integral equation method for general viscoelastic analysis. Int. J. Solids Struct. 39, 2643–2664.

Mesquita, A.D., Coda, H.B., Venturini, W.S., 2001. Alternative time marching process for BEM and FEM viscoelastic analysis. Int. J. Numer. Methods Eng. 51, 1157–1173.

Panagiotopoulos, C.G., 2009. Open BEM Project, Open Boundary Element Method Project. <http://www.openbemproject.org>.

Panagiotopoulos, C.G., Mantič, V., García, I.G., Graciani, E., 2013a. Quadratic programing for minimization of the total potential energy to solve contact problems using the collocation BEM. In: Sellier, A., Aliabadi, M., (Ed.), Advances in Boundary Element Techniques & Meshless Techniques XIV. EC, Eastleigh, pp. 292–297.

Panagiotopoulos, C.G., Mantič, V., Roubíček, T., 2013b. BEM solution of delamination problems using an interface damage and plasticity model. Comput. Mech. 51, 505–521.

París, F., Cañas, J., 1997. Boundary Element Method, Fundamentals and Applications. Oxford University Press, Oxford.
Rizzo, F.J., Shippy, D.J., 1971. An application of the correspondence principle of linear viscoelasticity theory. SIAM J. Appl. Math. 21, 321–330.
Roubíček, T., 2013a. Nonlinear Partial Differential Equations with Applications, second ed. Birkhäuser Verlag, Basel.
Roubíček, T., 2013b. Adhesive contact of visco-elastic bodies and defect measures arising by vanishing viscosity. SIAM J. Math. Anal. 45, 101–126.
Roubíček, T., Panagiotopoulos, C.G., Mantič, V., 2013. Quasistatic adhesive contact of visco-elastic bodies and its numerical treatment for very small viscosity. Z. Angew. Math. Mech. 93, 823–840.
Schanz, M., 1999. A boundary element formulation in time domain for viscoelastic solids. Commun. Numer. Methods Eng. 15, 799–809.
Schanz, M., Antes, H., Rüberg, T., 2005. Convolution quadrature boundary element method for quasi-static visco- and poroelastic continua. Comput. Struct. 83, 673–684.
Sládek, J., Sumec, J., Sládek, V., 1984. Viscoelastic crack analysis by the boundary integral equation method. Ing. Arch. 54, 275–282.
Syngellakis, S., Wu, J., 2004. Evaluation of various schemes for quasi-static boundary element analysis of polymers. Eng. Anal. Boundary Elem. 28, 733–745.
Zhu, X.Y., Chen, W.Q., Huang, Z.Y., Liu, Y.J., 2011. A fast multipole boundary element method for 2D viscoelastic problems. Eng. Anal. Boundary Elem. 35, 170–178.